Supporting Information

Regulating the Single-Molecule Magnetic Properties of Phenol Oxygen Bridged Binuclear Lanthanide Complexes through the Electronic and Spatial Effect of the Substituents

Xiang-Wen Liu,[a] Zhuo Wu,[a] Ji-Tun Chen,[a] Li Li,[b] Peng Chen,*[a] and Wen-Bin Sun*[a]

a. Key Laboratory of Functional Inorganic Material Chemistry Ministry of Education, School of Chemistry and Material Science Heilongjiang University, 74 Xuefu Road, Harbin 150080, P. R. China.

[b.]State Key Laboratory of Inorganic Synthesis and Preparative Chemistry, College of Chemistry, Jilin University, 2699 Qianjin Street, Changchun 130012, People's Republic of China

E-mail: wenbinsun@126.com

Table S1. Crystallographic data for **1**-**5**.

Complex	**1**	**2**	**3**	**4**	**5**
Empirical formula	$C_{78}H_{64}Dy_2F_{12}O_{15}$	$C_{76}H_{54}Dy_2F_{12}O_{18}$	$C_{60}H_{46}Dy_2F_{12}O_{18}$	$C_{52}H_{38}Dy_2F_{12}O_{18}S_4$	$C_{74}H_{50}Dy_2F_{12}O_{16}$
FW (g mol^{-1})	1794.29	1808.19	1607.97	1632.06	1748.14
Crystal system	Triclinic	Triclinic	Monoclinic	Monoclinic	Triclinic
Space group	*P*$\bar{1}$	*P*$\bar{1}$	*C*2/*c*	$P2_1/c$	*P*$\bar{1}$
Temperature (K)	293	298.0	298.0	296.15	298.0
a (Å)	10.8548(4)	11.9310(7)	11.9773(6)	11.6988(14)	10.8903(5)
b (Å)	13.8922(6)	13.3225(10)	24.0753(19)	23.426(3)	13.1650(7)
c (Å)	14.6209(6)	14.1270(10)	22.8685(14)	11.9469(14)	13.2667(7)
α (°)	117.058(4)	116.718(8)	90.00	90.00	69.817(5)
β (°)	91.633(3)	91.465(5)	96.255(6)	109.7750(10)	72.822(4)
γ (°)	110.919(3)	111.980(6)	90.00	90.00	74.762(4)
V (Å3)	1785.09(13)	1808.4(2)	6555.0(7)	3081.1(6)	1677.93(15)
ρ_{cacd} (Mg.m^{-3})	1.669	1.660	1.629	1.759	1.730
μ (mm^{-1})	11.932	2.152	2.363	2.645	2.314
F (000)	892.0	894.0	3160.0	1596.0	862.0
Independent relections	7059	9022	8205	6171	8298
Rint	0.0531	0.0341	0.0381	0.0457	0.0213
R1 [I > 2σ(I)]	0.0589	0.0549	0.0551	0.0447	0.0388
wR2 (all data)	0.1759	0.1118	0.1327	0.1218	0.0938
Goodness of fit on F^2	1.098	1.005	1.026	1.030	1.042
CCDC numbers	1957973	1957974	1957975	1957976	1957977

Table S2. Selected bond lengths (Å) and angles (°) for **1**

Dy1-Dy1’	3.8062(8)	Dy1-O1	2.303(5)	Dy1-O1’	2.275(5)	Dy1-O7’	2.673(5)
Dy1-O3	2.314(5)	Dy1-O5	2.306(5)	Dy1-O6	2.327(6)	Dy1-O4	2.286(5)
Dy1-O2	2.612(6)	O1-Dy1’	2.275(5)				
O1-Dy1-Dy1’	33.52(12)	O1’-Dy1-Dy1’	33.98(12)	O1’- Dy1-O1	67.5(2)	O1- Dy1-O7’	128.15(17)
O1’-Dy1-O7’	64.54(17)	O1’- Dy1-O3	86.23(19)	O1- Dy1-O3	83.23(18)	O1- Dy1-O5	129.8(2)
O1’- Dy1-O5	87.9(2)	O1- Dy1-O6	81.0(2)	O1’- Dy1-O6	115.8(2)	O1’- Dy1-O4	140.5(2)
O1’- Dy1-O2	129.76(19)	O1- Dy1-O2	64.21(18)	O7’- Dy1-Dy1’	96.70(12)	O3- Dy1- Dy1’	83.65(13)
O3- Dy1-O7’	75.26(18)	O3- Dy1-O6	144.8(2)	O3- Dy1-O2	75.4(2)	O5- Dy1- Dy1’	111.43(18)

O5- Dy1-O7′	66.70(19)	O5- Dy1-O3	140.2(2)	O5- Dy1-O6	71.4(2)	O5- Dy1-O2	134.6(3)
O6- Dy1- Dy1′	99.51(16)	O6- Dy1-O7′	138.0(2)	O6- Dy1-O2	69.4(3)	O4- Dy1- Dy1′	157.42(16)
O4- Dy1-O1	139.8(2)	O4- Dy1-O7′	77.4(2)	O4- Dy1-O3	73.8(2)	O4- Dy1-O5	86.5(2)
O4- Dy1-O6	99.2(2)	O4- Dy1-O2	78.2(2)	O2- Dy1- Dy1′	96.84(14)	O2- Dy1-O7′	145.9(2)
Dy1′- O1- Dy1	112.5(2)						

Table S3. Selected bond lengths (Å) and angles (°) for **2**

Dy1-Dy1′	3.8562(7)	Dy1-O1	2.294(3)	Dy1-O1′	2.317(3)	Dy1-O7′	2.596(3)
Dy1-O3	2.293(4)	Dy1-O5	2.289(4)	Dy1-O6	2.307(4)	Dy1-O4	2.280(3)
Dy1-O2	2.629(3)	O1-Dy1′	2.317(3)				
O1-Dy1-Dy1′	33.43(8)	O1′-Dy1-Dy1′	33.06(8)	O1- Dy1-O1′	66.49(13)	O1- Dy1-O7′	128.61(11)
O1′-Dy1-O7′	63.95(10)	O1′- Dy1-O3	85.03(13)	O1- Dy1-O3	85.42(13)	O1- Dy1-O5	88.07(13)
O1′- Dy1-O5	131.43(13)	O1- Dy1-O6	116.09(13)	O6- Dy1-O1′	82.49(13)	O4- Dy1-O1′	139.38(12)
O1′- Dy1-O2	126.83(12)	O1- Dy1-O2	64.50(11)	O7′- Dy1-Dy1′	96.17(7)	O3- Dy1- Dy1′	84.29(9)
O3- Dy1-O7′	77.77(12)	O3- Dy1-O6	147.64(13)	O3- Dy1-O2	71.93(12)	O5- Dy1- Dy1′	112.17(11)
O5- Dy1-O7′	136.13(14)	O5- Dy1-O3	135.54(15)	O5- Dy1-O6	72.38(14)	O5- Dy1-O2	65.64(14)
O6- Dy1- Dy1′	100.56(10)	O6- Dy1-O7′	69.92(12)	O6- Dy1-O2	138.01(13)	O4- Dy1- Dy1′	158.96(10)
O4- Dy1-O1	143.35(13)	O4- Dy1-O7′	77.35(12)	O4- Dy1-O3	74.80(14)	O4- Dy1-O5	85.15(14)
O4- Dy1-O6	95.98(14)	O4- Dy1-O2	79.98(12)	O2- Dy1- Dy1′	95.97(8)	O7′- Dy1-O2	145.93(11)
Dy1′- O1- Dy1	113.51(13)						

Table S4. Selected bond lengths (Å) and angles (°) for **3**

Dy1-Dy1′	3.8667(6)	Dy1-O1	2.283(4)	Dy1-O1′	2.334(3)	Dy1-O7′	2.594(4)
Dy1-O3	2.304(4)	Dy1-O5	2.301(5)	Dy1-O6	2.297(5)	Dy1-O4	2.277(4)
Dy1-O2	2.570(4)	O1-Dy1′	2.334(3)				
O1-Dy1-Dy1′	33.55(8)	O1′-Dy1-Dy1′	32.72(9)	O1- Dy1-O1′	66.27(14)	O1- Dy1-O7′	130.67(12)
O1′-Dy1-O7′	64.84(13)	O3- Dy1-O1′	84.10(13)	O1- Dy1-O3	90.92(14)	O1- Dy1-O5	94.85(18)
O5- Dy1-O1′	137.20(16)	O1- Dy1-O6	105.28(15)	O6- Dy1-O1′	77.16(16)	O4- Dy1-O1′	138.48(14)

O1'- Dy1-O2	126.12(14)	O1- Dy1-O2	65.04(13)	O7'- Dy1-Dy1'	97.36(9)	O3- Dy1- Dy1'	86.98(10)
O3- Dy1-O7'	78.11(14)	O6-Dy1-O3	147.35(16)	O3- Dy1-O2	75.09(15)	O5- Dy1- Dy1'	119.53(13)
O5- Dy1-O7'	125.96(19)	O5- Dy1-O3	136.42(16)	O6- Dy1-O5	71.30(18)	O5- Dy1-O2	68.61(19)
O6- Dy1- Dy1'	91.23(13)	O6- Dy1-O7'	69.80(16)	O6- Dy1-O2	137.41(17)	O4- Dy1- Dy1'	160.34(11)
O4- Dy1-O1	146.03(14)	O4- Dy1-O7'	76.41(14)	O4- Dy1-O3	73.53(15)	O4- Dy1-O5	78.01(17)
O4- Dy1-O6	103.69(17)	O4- Dy1-O2	81.63(14)	O2- Dy1- Dy1'	96.13(10)	O2- Dy1-O7'	149.19(14)
Dy1'- O1- Dy1	113.73(14)						

Table S5. Selected bond lengths (Å) and angles (°) for **4**

Dy1-Dy1'	3.8511(6)	Dy1-O1	2.310(4)	Dy1-O1'	2.322(4)	Dy1-O7'	2.610(4)
Dy1-O3	2.305(4)	Dy1-O5	2.324(5)	Dy1-O6	2.274(4)	Dy1-O4	2.258(4)
Dy1-O2	2.676(4)	O1-Dy1'	2.322(4)				
O1-Dy1-Dy1'	33.85(10)	O1'-Dy1-Dy1'	33.66(9)	O1- Dy1-O1'	67.51(16)	O1- Dy1-O7'	126.06(14)
O1'-Dy1-O7'	63.00(13)	O3- Dy1-O1'	91.45(14)	O3- Dy1-O1	88.46(14)	O1- Dy1-O5	134.26(17)
O1'- Dy1-O5	89.18(17)	O6- Dy1-O1	79.21(15)	O6- Dy1-O1'	109.39(15)	O4- Dy1-O1'	148.22(15)
O1'- Dy1-O2	130.43(13)	O1- Dy1-O2	63.92(13)	O7'- Dy1-Dy1'	94.55(9)	O3- Dy1- Dy1'	89.95(10)
O3- Dy1-O7'	73.02(15)	O6-Dy1-O3	148.98(17)	O3- Dy1-O2	78.11(14)	O5- Dy1- Dy1'	114.21(14)
O5- Dy1-O7'	65.39(16)	O3- Dy1-O5	132.69(16)	O6- Dy1-O5	72.14(17)	O5- Dy1-O2	132.82(16)
O6- Dy1- Dy1'	95.04(12)	O6- Dy1-O7'	136.67(16)	O6- Dy1-O2	70.89(16)	O4- Dy1- Dy1'	163.35(12)
O4- Dy1-O1	137.96(15)	O4- Dy1-O7'	85.53(15)	O4- Dy1-O3	74.11(15)	O4- Dy1-O5	80.99(18)
O4- Dy1-O6	96.28(17)	O4- Dy1-O2	75.03(15)	O2- Dy1- Dy1'	97.31(9)	O7'- Dy1-O2	148.70(14)
Dy1'- O1- Dy1	112.49(16)						

Table S6. Selected bond lengths (Å) and angles (°) for **5**

Dy1-Dy1'	3.8659(5)	Dy1-O1	2.284(3)	Dy1-O1'	2.348(3)	Dy1-O7'	2.570(3)
Dy1-O3	2.320(3)	Dy1-O5	2.290(3)	Dy1-O6	2.300(3)	Dy1-O4	2.286(3)
Dy1-O2	2.616(3)	O1-Dy1'	2.348(3)				
O1-Dy1-Dy1'	33.95(6)	O1'-Dy1-Dy1'	32.91(7)	O1- Dy1-O1'	66.86(11)	O1- Dy1-O7'	131.13(10)

O1'-Dy1-O7'	64.86(10)	O3- Dy1-O1'	81.00(9)	O1- Dy1-O3	87.26(10)	O1- Dy1-O5	94.50(11)
O5- Dy1-O1'	137.65(10)	O1- Dy1-O6	103.97(11)	O6- Dy1-O1'	76.01(9)	O4- Dy1-O1'	138.10(10)
O1'- Dy1-O2	126.21(9)	O1- Dy1-O2	64.43(9)	O7'- Dy1-Dy1'	97.51(7)	O3- Dy1- Dy1'	82.92(7)
O3- Dy1-O7'	78.37(11)	O6-Dy1-O3	147.60(11)	O3- Dy1-O2	75.35(10)	O5- Dy1- Dy1'	119.68(9)
O5- Dy1-O7'	126.78(11)	O5- Dy1-O3	138.09(10)	O5- Dy1-O6	72.18(10)	O5- Dy1-O2	67.99(10)
O6- Dy1- Dy1'	89.76(8)	O6- Dy1-O7'	71.34(10)	O6- Dy1-O2	136.96(10)	O4- Dy1- Dy1'	156.58(7)
O1- Dy1-O4	142.00(10)	O4- Dy1-O7'	77.53(10)	O4- Dy1-O3	73.66(10)	O4- Dy1-O5	79.86(11)
O4- Dy1-O6	109.71(11)	O4- Dy1-O2	78.88(11)	O2- Dy1- Dy1'	95.95(7)	O7'- Dy1-O2	148.63(10)
Dy1'- O1- Dy1	113.14(11)						

Table S7. Continuous Shape Measures (CShMs) of the coordination geometry for Dy(III) ion in compounds **1–5** (S values calculated with the Shape program). The S values indicated the proximity to the ideal polyhedron, thus, *S* = 0 corresponds to the non-distorted polyhedron. The three closer ideal geometries to the real complexes are listed and below are the symmetry and description for each polyhedron.

Complex	s	Polyhedron		
Complex 1	2.312	JBTPR-8	C2v	Biaugmented trigonal prism J50
	2.553	BTPR-8	C2v	Biaugmented trigonal prism
	3.149	TDD-8	D2d	Triangular dodecahedron
Complex 2	2.344	JBTPR-8	C2v	Biaugmented trigonal prism J50
	2.465	BTPR-8	C2v	Biaugmented trigonal prism
	3.255	TDD-8	D2d	Triangular dodecahedron
Complex 3	2.933	BTPR-8	C2v	Biaugmented trigonal prism
	3.066	TDD-8	D2d	Triangular dodecahedron
	3.180	JBTPR-8	C2v	Biaugmented trigonal prism J50
Complex 4	3.125	JBTPR-8	C2v	Biaugmented trigonal prism J50
	3.372	TDD-8	D2d	Triangular dodecahedron
	3.373	BTPR-8	C2v	Biaugmented trigonal prism
Complex 5	2.356	BTPR-8	C2v	Biaugmented trigonal prism
	2.617	JBTPR-8	C2v	Biaugmented trigonal prism J50
	3.036	TDD-8	D2d	Triangular dodecahedron

Table S8. Parameters used to fit the Arrhenius plots from Fig. 4 using approximations.

$1/\tau = 1/\tau_{QTM} + CT^{n} + \tau_0^{-1}\exp(-U_{eff}/K_BT)$ (1):

Zero dc field	1	2	3	4	5
τ_{QTM}^{-1}/s^{-1}	2.0×10^{-2}	1.9×10^{-1}	3.8×10^{-2}	1.3×10^{-3}	8.7×10^{-1}
$C/s^{-1}k^{-n}$	6.3	5.6×10^{-2}	4.0	53.8	3.2×10^{-3}
n	2.2	3.5	2.7	2.3	5.2
τ_0/s	8.8×10^{-6}	9.3×10^{-8}	9.8×10^{-6}	9.6×10^{-6}	1.1×10^{-7}
U/k	39.5	106.6	45.0	22.8	115.1

$1/\tau = CT^{n} + \tau_0^{-1}\exp(-U_{eff}/K_BT)$ (2):

Optimum field	1	2	3	4	5
$C/s^{-1}k^{-n}$	8.1	1.4×10^{-1}	1.1	50.4	4.7×10^{-3}
n	1.8	3.1	3.2	1.7	5.0
τ_0/s	3.9×10^{-6}	7.4×10^{-8}	5.6×10^{-6}	3.3×10^{-6}	4.5×10^{-8}
U/k	41.9	108.7	46.9	24.5	125.1

Table S9. Best fitted parameters (χ_T, χ_S, τ and α) with the extended Debye model for compound **1** under zero field in the temperature range 2-10 K.

T/ K	χ_S / $cm^3\ mol^{-1}$	χ_T / $cm^3\ mol^{-1}$	τ/s	α	R
2	0.69974	4.70125	0.01240	0.29545	3.19×10^{-4}
3	0.66790	4.34042	0.00841	0.26062	2.38×10^{-4}
4	0.64770	3.78169	0.00533	0.22782	2.60×10^{-4}
5	0.59980	3.28933	0.00311	0.21018	2.60×10^{-4}
6	0.66374	2.90760	0.00191	0.18984	2.81×10^{-4}
7	0.73834	2.58599	0.00115	0.18695	2.14×10^{-4}
8	0.88934	2.33133	0.00069	0.18448	1.87×10^{-4}
9	1.10000	2.11986	0.00042	0.19022	1.51×10^{-4}
10	1.29864	1.95400	0.00024	0.19816	3.05×10^{-4}

Table S10. Best fitted parameters (χ_T, χ_S, τ and α) with the extended Debye model for compound **2** under zero field in the temperature range 3-13 K.

T/ K	χ_S / cm^3 mol^{-1}	χ_T / cm^3 mol^{-1}	τ/s	α	R
3	0.42718	4.29415	0.10010	0.18195	3.84×10^{-3}
4	0.34301	4.10906	0.09059	0.21698	8.24×10^{-4}
5	0.31870	3.35034	0.04740	0.17123	4.78×10^{-4}
6	0.28889	2.88759	0.02587	0.15412	2.85×10^{-4}
7	0.27026	2.53023	0.01415	0.13797	1.68×10^{-4}
8	0.25421	2.25992	0.00800	0.13356	1.14×10^{-4}
9	0.24429	2.05433	0.00456	0.14269	1.15×10^{-4}
10	0.27586	1.85388	0.00245	0.12983	1.66×10^{-4}
11	0.24188	1.71062	0.00119	0.17533	8.94×10^{-5}
12	0.22397	1.58668	0.00052	0.22027	1.04×10^{-4}
13	0.28000	1.47274	0.00024	0.21092	1.09×10^{-4}

Table S11. Best fitted parameters (χ_T, χ_S, τ and α) with the extended Debye model for compound **3** under zero field in the temperature range 2-12 K.

T/ K	χ_S / cm^3 mol^{-1}	χ_T / cm^3 mol^{-1}	τ/s	α	R
2	0.13127	4.90089	0.01668	0.20765	4.01×10^{-4}
3	0.11938	4.30523	0.00964	0.18528	2.46×10^{-4}
4	0.10152	3.67367	0.00485	0.18042	1.55×10^{-4}
5	0.10033	3.16597	0.00248	0.19330	1.96×10^{-4}
6	0.20373	2.76351	0.00129	0.19153	2.58×10^{-4}
7	0.36884	2.45525	0.00070	0.20411	1.98×10^{-4}
8	0.70024	2.19866	0.00047	0.17812	8.77×10^{-5}
9	0.98591	1.98811	0.00041	0.12145	3.33×10^{-5}
10	1.11152	1.81680	0.00033	0.08145	3.58×10^{-5}
11	1.19123	1.67471	0.00025	0.04559	3.74×10^{-5}
12	1.25186	1.55051	0.00020	0.00215	4.56×10^{-5}

Table S12. Best fitted parameters (χ_T, χ_S, τ and α) with the extended Debye model for compound **4** under zero field in the temperature range 2-6 K.

T/ K	χ_S / cm^3 mol^{-1}	χ_T / cm^3 mol^{-1}	τ/s	α	R
2	0.46727	4.62008	0.00099	0.20535	1.29×10^{-4}
2.5	0.48474	4.40832	0.00083	0.20117	9.12×10^{-5}
3	0.52829	4.10898	0.00068	0.19843	6.56×10^{-5}
3.5	0.57494	3.80431	0.00054	0.19645	4.94×10^{-5}
4	0.65470	3.51896	0.00043	0.19282	4.32×10^{-5}
4.5	0.72860	3.26193	0.00033	0.19904	4.05×10^{-5}
5	0.90880	3.04062	0.00028	0.19246	3.22×10^{-5}
5.5	1.18923	2.83579	0.00025	0.15803	3.08×10^{-5}
6	1.40000	2.65784	0.00022	0.14863	3.43×10^{-5}

Table S13. Best fitted parameters (χ_T, χ_S, τ and α) with the extended Debye model for compound **5** under zero field in the temperature range 5-13 K.

T/ K	χ_S / cm^3 mol^{-1}	χ_T / cm^3 mol^{-1}	τ/s	α	R
5	0.33474	4.51221	0.06466	0.09596	2.68×10^{-4}
6	0.27991	3.86424	0.02477	0.07706	1.95×10^{-4}
7	0.27509	3.39014	0.01093	0.05653	7.14×10^{-5}
8	0.25354	3.03026	0.00540	0.04831	4.34×10^{-5}
9	0.25377	2.74297	0.00288	0.04033	4.38×10^{-5}
10	0.25573	2.50978	0.00160	0.03254	3.11×10^{-5}
11	0.26377	2.31203	0.00091	0.03051	2.43×10^{-5}
12	0.25884	2.13850	0.00051	0.03947	4.02×10^{-5}
13	0.26000	2.00000	0.00027	0.05188	8.98×10^{-5}

Table S14. Best fitted parameters (χ_T, χ_S, τ and α) with the extended Debye model for compound **1** under 500 Oe in the temperature range 2-10 K.

T/ K	χ_S / cm^3 mol^{-1}	χ_T / cm^3 mol^{-1}	τ/s	α	R
2	0.84289	7.04084	0.03208	0.29995	8.51×10^{-4}
3	0.79742	6.54098	0.01810	0.28418	4.11×10^{-4}
4	0.83266	5.49915	0.00824	0.22263	4.08×10^{-4}
5	0.79438	4.85268	0.00417	0.21593	2.26×10^{-4}
6	0.76734	4.30050	0.00208	0.21753	2.27×10^{-4}
7	0.94678	3.79693	0.00118	0.20025	1.70×10^{-4}
8	1.15199	3.43356	0.00066	0.20247	1.22×10^{-4}
9	1.53134	3.10000	0.00039	0.17642	9.12×10^{-5}
10	2.00331	2.83110	0.00030	0.11476	6.97×10^{-5}

Table S15. Best fitted parameters (χ_T, χ_S, τ and α) with the extended Debye model for compound **2** under 1100 Oe in the temperature range 4-13 K.

T/ K	χ_S / cm^3 mol^{-1}	χ_T / cm^3 mol^{-1}	τ/s	α	R
4	0.28072	5.70000	0.08873	0.29325	5.57×10^{-4}
5	0.28522	4.66885	0.04305	0.22438	4.34×10^{-4}
6	0.28555	3.99149	0.02263	0.17960	3.33×10^{-4}
7	0.27238	3.49066	0.01241	0.15388	2.15×10^{-4}
8	0.26925	3.10065	0.00701	0.13395	1.65×10^{-4}
9	0.26971	2.80606	0.00406	0.13305	1.32×10^{-4}
10	0.31126	2.56673	0.00230	0.13565	2.00×10^{-4}
11	0.27567	2.35425	0.00113	0.16869	1.08×10^{-4}
12	0.24264	2.17379	0.00051	0.20703	2.04×10^{-4}
13	0.34767	2.01855	0.00024	0.19928	1.06×10^{-4}

Table S16. Best fitted parameters (χ_T, χ_S, τ and α) with the extended Debye model for compound **3** under 900 Oe in the temperature range 2-12 K.

T/ K	χ_S / cm^3 mol^{-1}	χ_T / cm^3 mol^{-1}	τ/s	α	R
2	0.05391	6.20000	0.08964	0.29893	7.59×10^{-4}

3	0.06674	5.34539	0.02999	0.25289	4.22×10^{-4}
4	0.07905	4.46720	0.00967	0.22146	3.44×10^{-4}
5	0.10341	3.84175	0.00378	0.21639	3.61×10^{-4}
6	0.19210	3.34872	0.00161	0.21378	3.71×10^{-4}
7	0.35000	2.97303	0.00076	0.22777	3.00×10^{-4}
8	0.84063	2.66348	0.00052	0.18566	1.29×10^{-4}
9	1.09870	2.40438	0.00039	0.16031	5.96×10^{-5}
10	1.29428	2.19682	0.00032	0.09773	3.72×10^{-5}
11	1.45586	2.02356	0.00027	0.02106	4.03×10^{-5}
12	1.48823	1.87827	0.00019	0.00765	6.28×10^{-5}

Table S17. Best fitted parameters (χ_T, χ_S, τ and α) with the extended Debye model for compound **4** under 1100 Oe in the temperature range 2-6 K.

T/ K	χ_S / cm^3 mol^{-1}	χ_T / cm^3 mol^{-1}	τ/s	α	R
2	0.43964	6.01480	0.00541	0.24205	6.45×10^{-4}
2.5	0.41880	5.57484	0.00372	0.25034	4.51×10^{-4}
3	0.39637	5.10784	0.00228	0.24670	2.78×10^{-4}
3.5	0.53049	4.67247	0.00141	0.22378	1.90×10^{-4}
4	0.43425	4.32223	0.00081	0.24456	1.49×10^{-4}
4.5	0.49953	4.00387	0.00049	0.25597	1.51×10^{-4}
5	0.95257	3.71045	0.00037	0.21500	5.30×10^{-5}
5.5	1.09615	3.46738	0.00025	0.22787	6.65×10^{-5}
6	1.50712	3.24564	0.00021	0.18353	3.83×10^{-5}

Table S18. Best fitted parameters (χ_T, χ_S, τ and α) with the extended Debye model for compound **5** under 1500 Oe in the temperature range 5-13 K.

T/ K	χ_S / cm^3 mol^{-1}	χ_T / cm^3 mol^{-1}	τ/s	α	R
5	0.18889	2.59735	0.06043	0.13677	3.88×10^{-4}
6	0.17565	2.21721	0.02283	0.08594	2.51×10^{-4}

7	0.16255	1.94564	0.01015	0.06007	1.33×10^{-4}
8	0.14678	1.74606	0.00507	0.05452	8.89×10^{-5}
9	0.14994	1.58113	0.00274	0.04654	7.19×10^{-5}
10	0.14783	1.44152	0.00152	0.03756	4.25×10^{-5}
11	0.15544	1.32655	0.00087	0.03053	3.72×10^{-5}
12	0.14684	1.22832	0.00049	0.03451	3.96×10^{-5}
13	0.20213	1.14353	0.00028	0.02076	2.87×10^{-5}

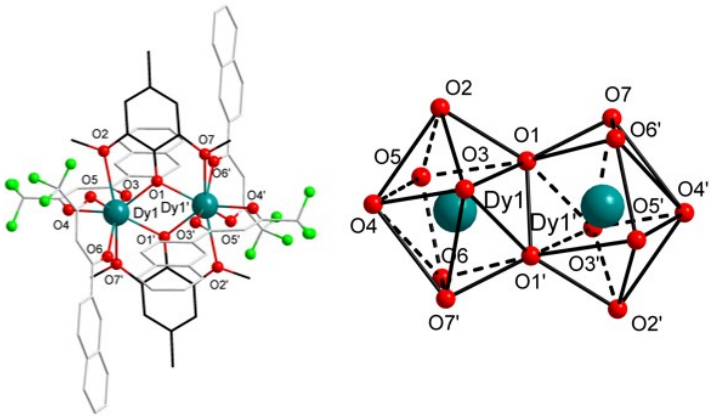

Fig. S1. The crystal structures and local coordination of complexes **1**. Hydrogen atoms are omitted for clarity.

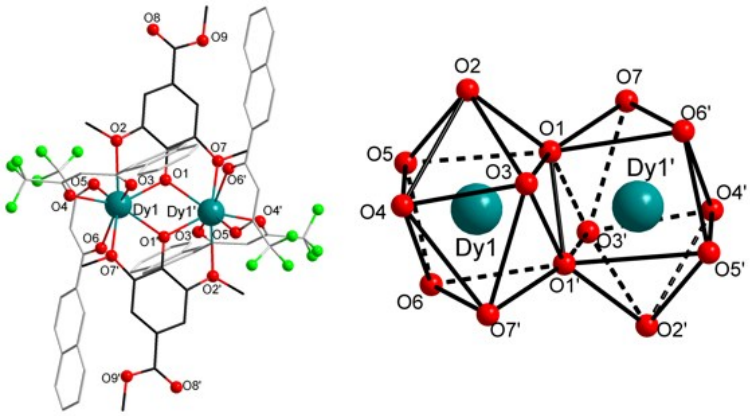

Fig. S2. The crystal structures and local coordination of complexes **2**. Hydrogen atoms are omitted for clarity.

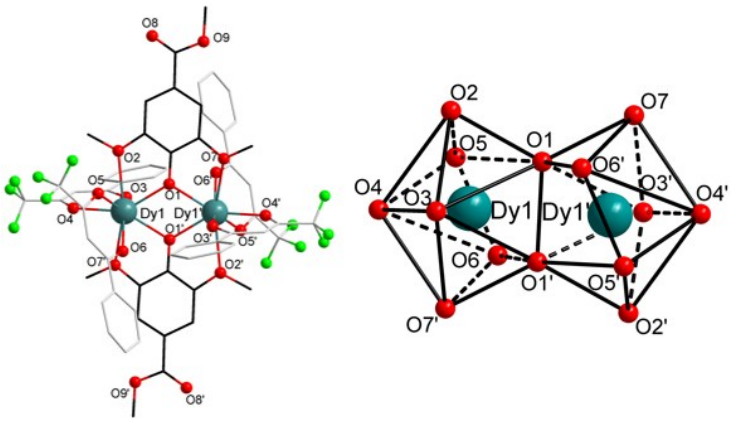

Fig. S3. The crystal structures and local coordination of complexes **3**. Hydrogen atoms are omitted for clarity.

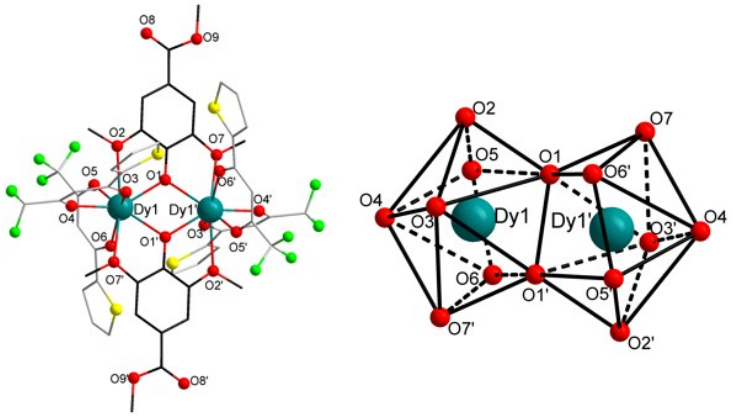

Fig. S4. The crystal structures and local coordination of complexes **4**. Hydrogen atoms are omitted for clarity.

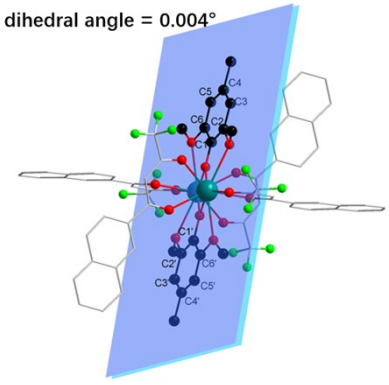

Fig. S5. The dihedral angle of the two benzene rings of the bridged ligand in complex **1**.

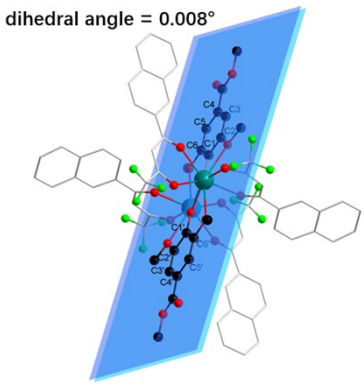

Fig. S6. The dihedral angle of the two benzene rings of the bridged ligand in complex **2**.

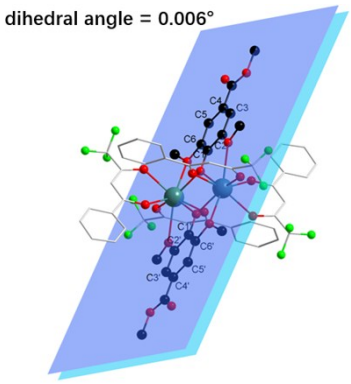

Fig. S7. The dihedral angle of the two benzene rings of the bridged ligand in complex **3**.

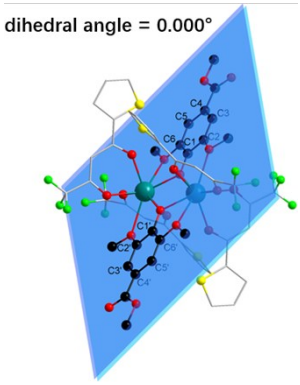

Fig. S8. The dihedral angle of the two benzene rings of the bridged ligand in complex **4**.

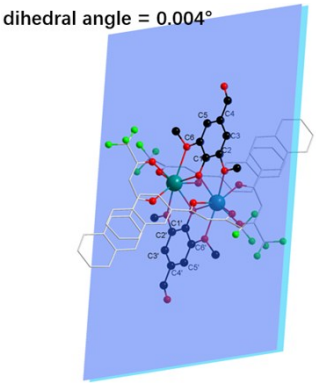

Fig. S9. The dihedral angle of the two benzene rings of the bridged ligand in complex **5**.

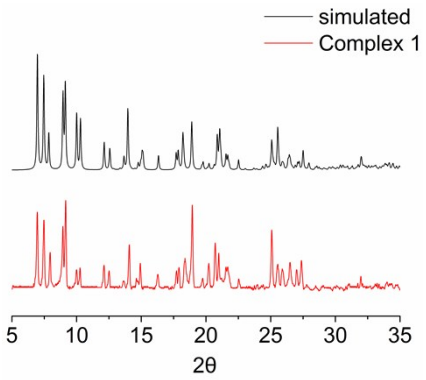

Fig. S10. PXRD analysis of complex **1**. The black line is simulated data from single crystal data.

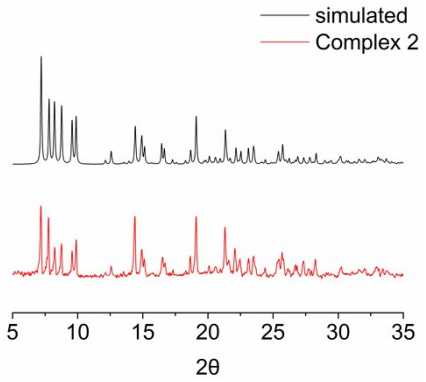

Fig. S11. PXRD analysis of complex **2**. The black line is simulated data from single crystal data.

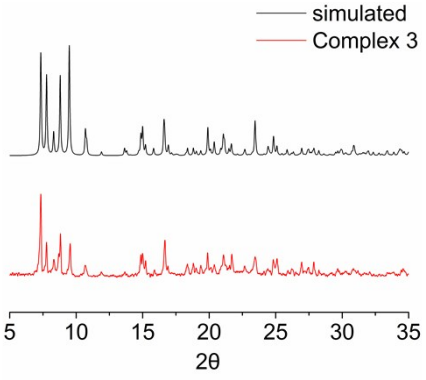

Fig. S12. PXRD analysis of complex **3**. The black line is simulated data from single crystal data.

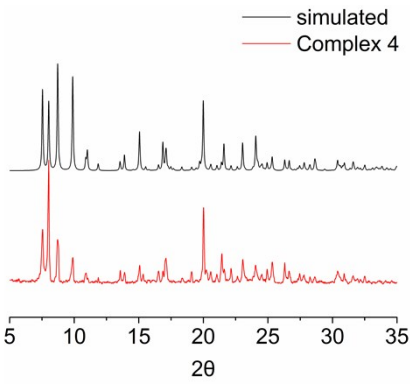

Fig. S13. PXRD analysis of complex **4**. The black line is simulated data from single crystal data.

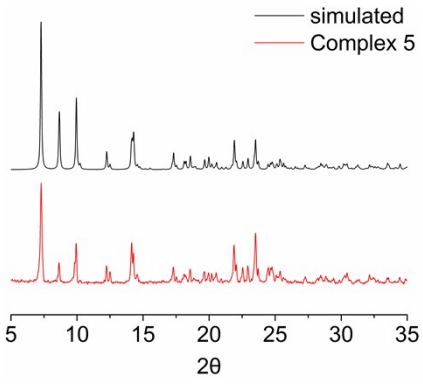

Fig. S14. PXRD analysis of complex **5**. The black line is simulated data from single crystal data.

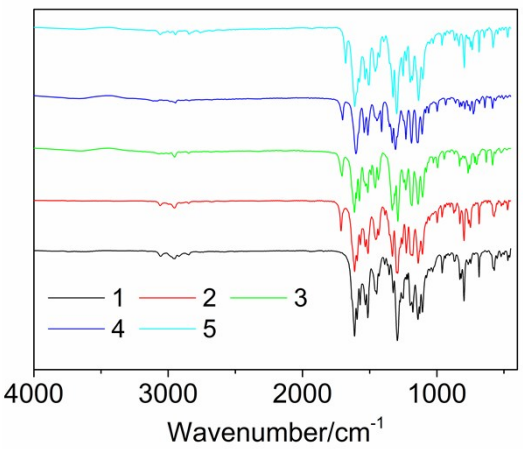

Fig. S15. FT-IR spectra of all the complexes.

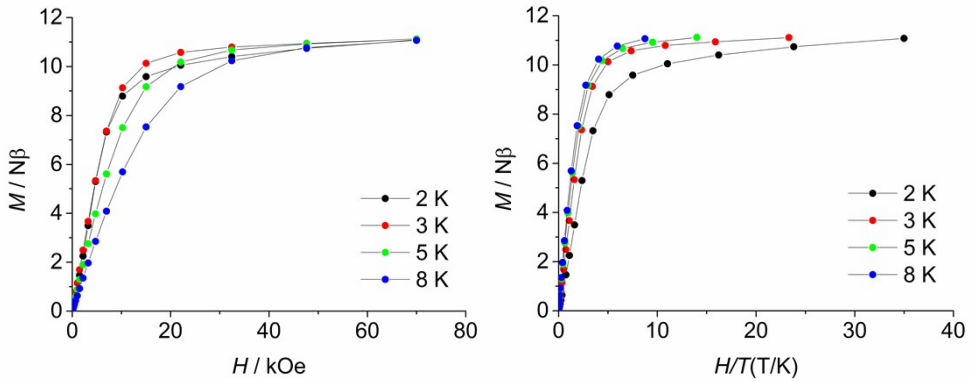

Fig. S16. The field dependence of magnetization (left) and magnetization data (right) for **1** at 2, 3, 5 and 8 K.

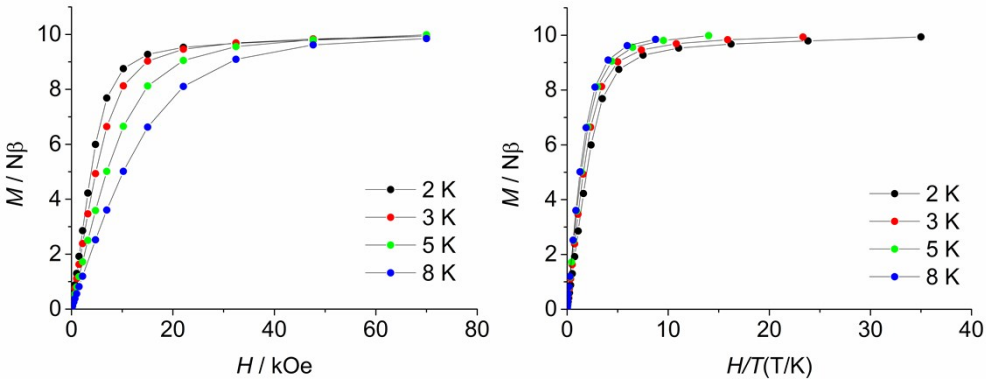

Fig. S17. The field dependence of magnetization (left) and magnetization data (right) for **2** at 2, 3, 5 and 8 K.

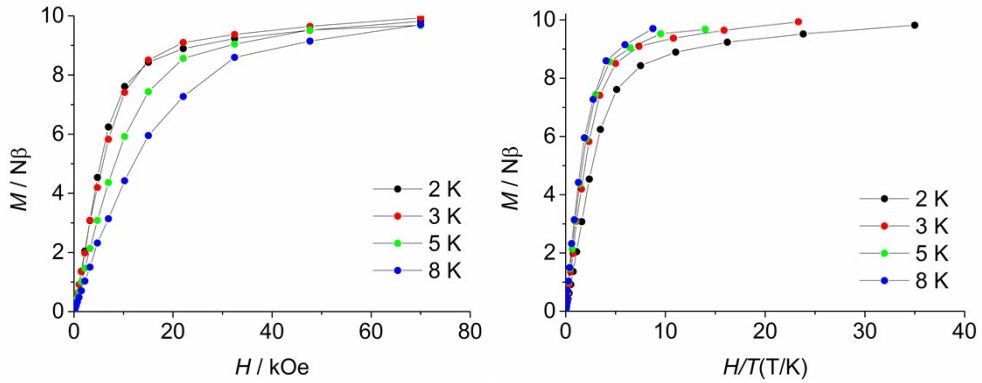

Fig. S18. The field dependence of magnetization (left) and magnetization data (right) for **3** at 2, 3, 5 and 8 K.

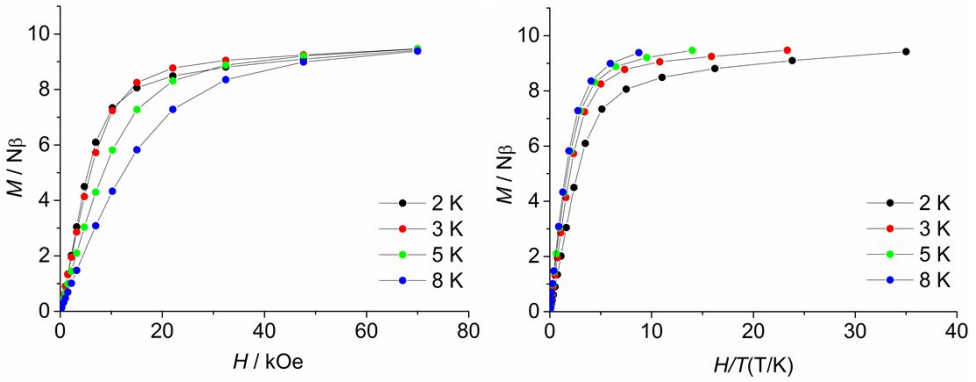

Fig. S19. The field dependence of magnetization (left) and magnetization data (right) for **4** at 2, 3, 5 and 8 K.

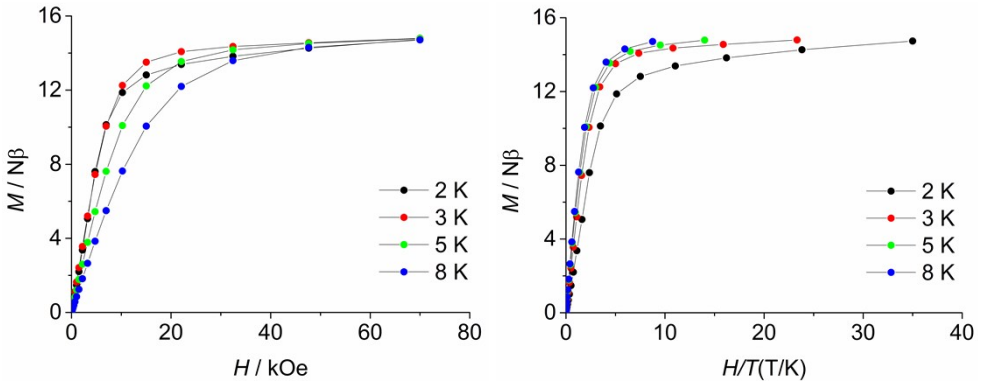

Fig. S20. The field dependence of magnetization (left) and magnetization data (right) for **5** at 2, 3, 5 and 8 K.

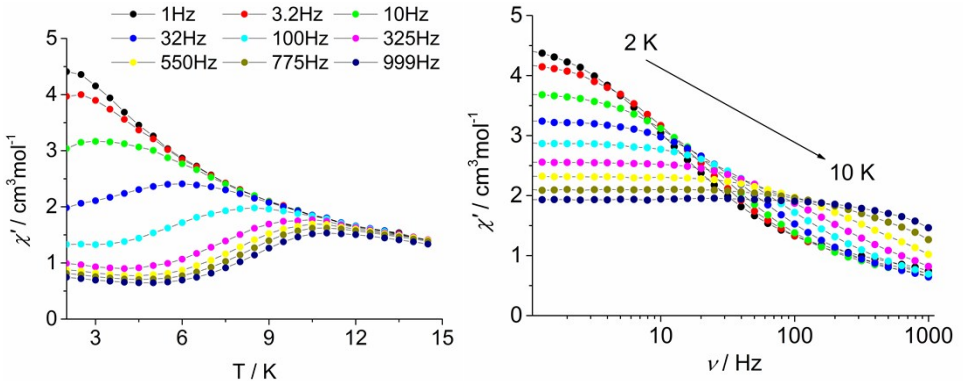

Fig. S21. Temperature dependence of the in-phase (χ') ac susceptibility (left) and frequency dependence of the in-phase (χ') ac susceptibility (right) of complex **1** under 0 Oe.

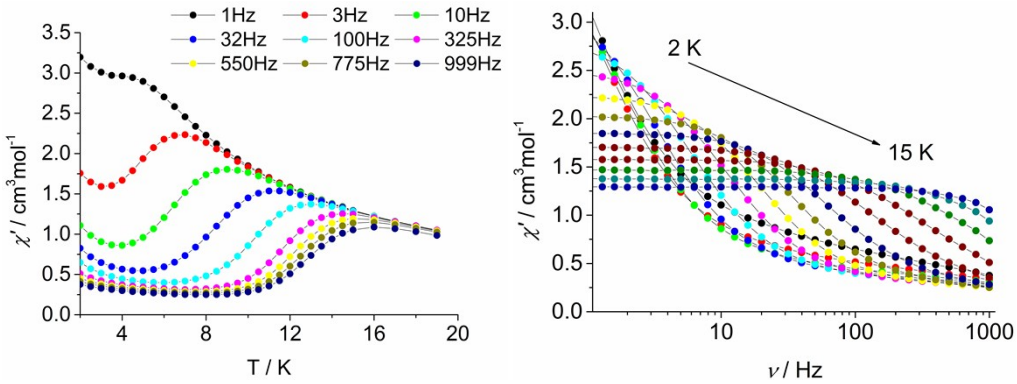

Fig. S22. Temperature dependence of the in-phase (χ') ac susceptibility (left) and frequency dependence of the in-phase (χ') ac susceptibility (right) of complex **2** under 0 Oe.

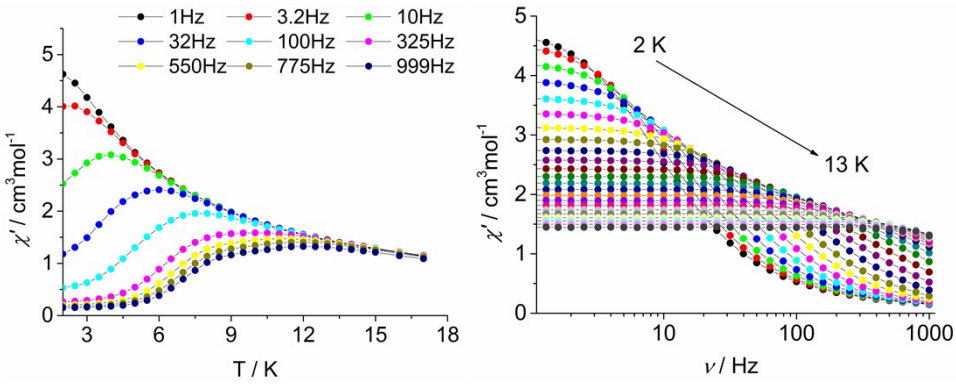

Fig. S23. Temperature dependence of the in-phase (χ') ac susceptibility (left) and frequency dependence of the in-phase (χ') ac susceptibility (right) of complex **3** under 0 Oe.

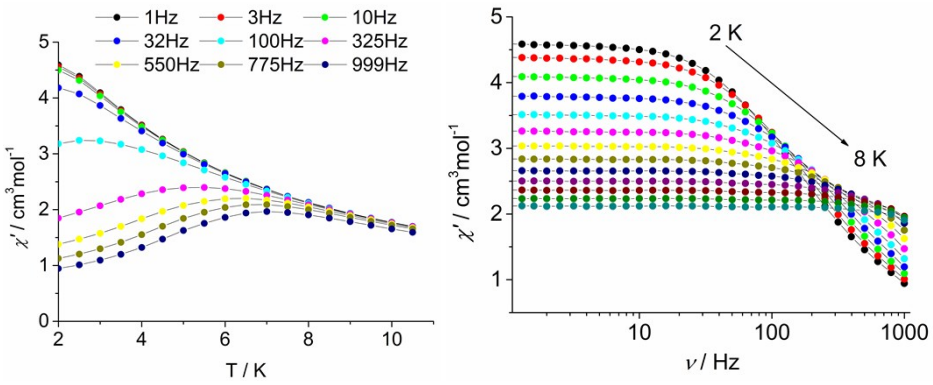

Fig. S24. Temperature dependence of the in-phase (χ') ac susceptibility (left) and frequency dependence of the in-phase (χ') ac susceptibility (right) of complex **4** under 0 Oe.

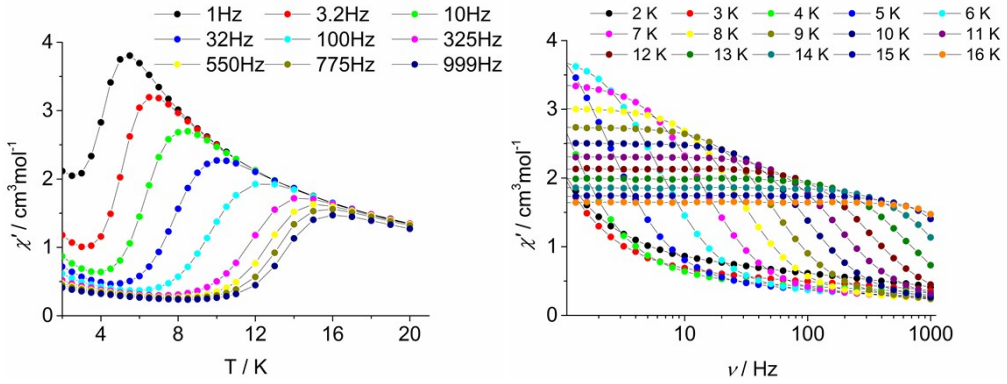

Fig. S25. Temperature dependence of the in-phase (χ') ac susceptibility (left) and frequency dependence of the in-phase (χ') ac susceptibility (right) of complex **5** under 0 Oe.

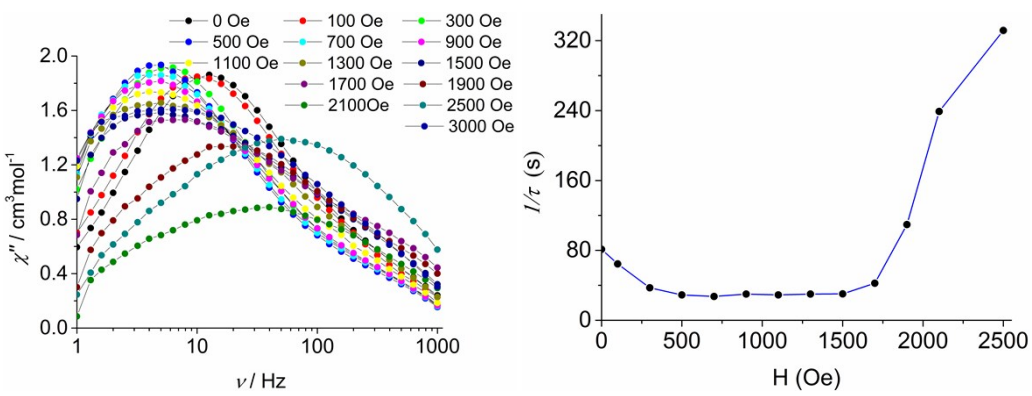

Fig. S26. Plot of the frequency dependence of the out-of-phase (χ'') ac susceptibility component under indicated dc field at 2 K for complex **1** (left). Plot of 1/*τ* vs. *H* for **1** under different dc fields at 2 K (right), the solid line is guide for eyes.

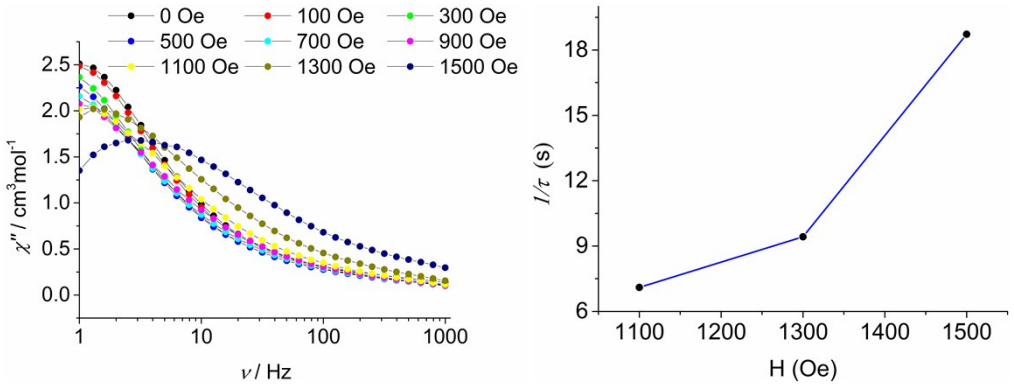

Fig. S27. Plot of the frequency dependence of the out-of-phase (χ'') ac susceptibility component under indicated dc field at 2 K for complex **2** (left). Plot of 1/*τ* vs. *H* for **2** under different dc fields at 2 K (right), the solid line is guide for eyes.

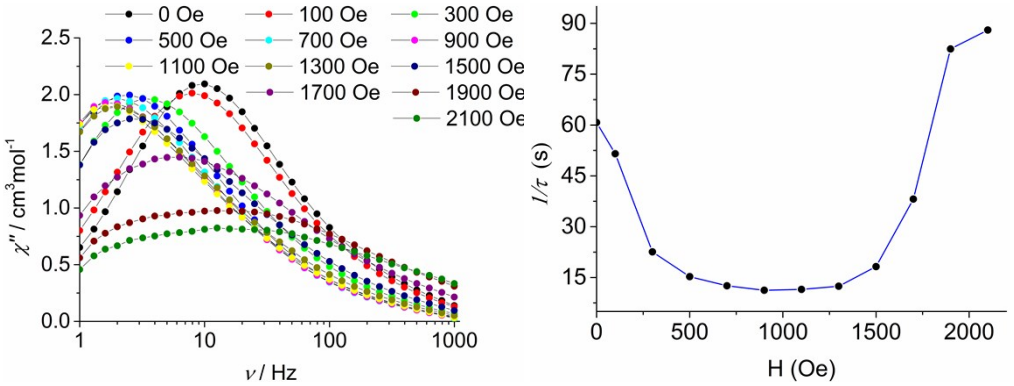

Fig. S28. Plot of the frequency dependence of the out-of-phase (χ'') ac susceptibility component under

indicated dc field at 2 K for complex **3** (left). Plot of 1/τ vs. *H* for **3** under different dc fields at 2 K (right), the solid line is guide for eyes.

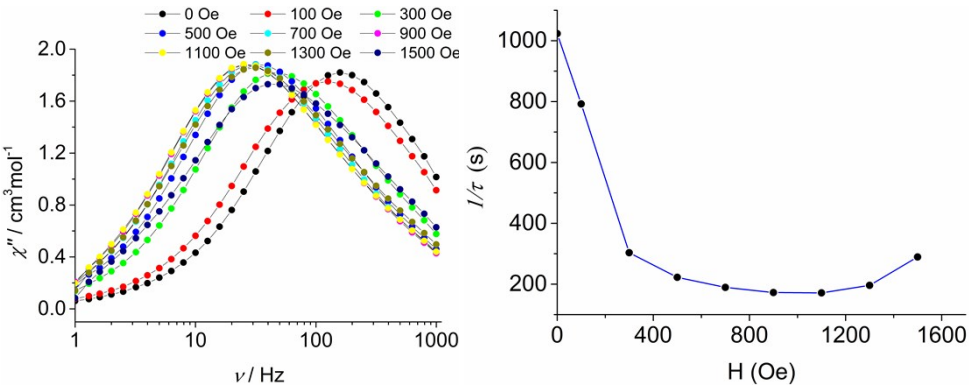

Fig. S29. Plot of the frequency dependence of the out-of-phase (χ'') ac susceptibility component under indicated dc field at 2 K for complex **4** (left). Plot of 1/τ vs. *H* for **4** under different dc fields at 2 K (right), the solid line is guide for eyes.

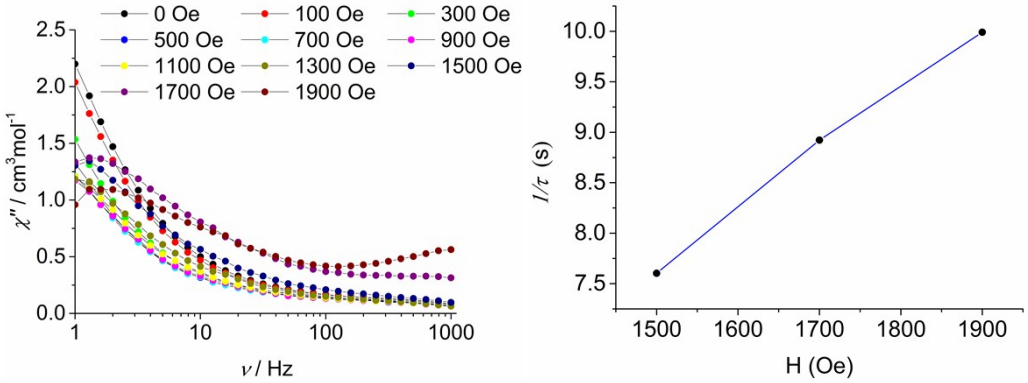

Fig. S30. Plot of the frequency dependence of the out-of-phase (χ'') ac susceptibility component under indicated dc field at 2 K for complex **5** (left). Plot of 1/τ vs. *H* for **5** under different dc fields at 2 K (right), the solid line is guide for eyes.

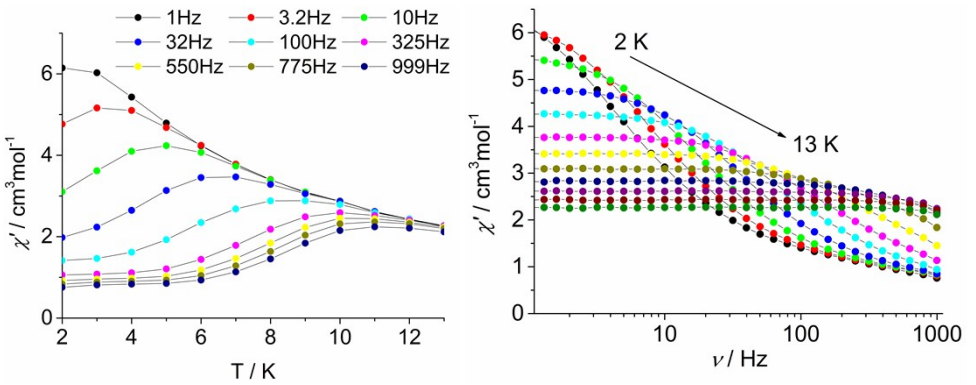

Fig. S31. Temperature dependence of the in-phase (χ') ac susceptibility (left) and frequency dependence of the in-phase (χ') ac susceptibility (right) of complex **1** under 500 Oe.

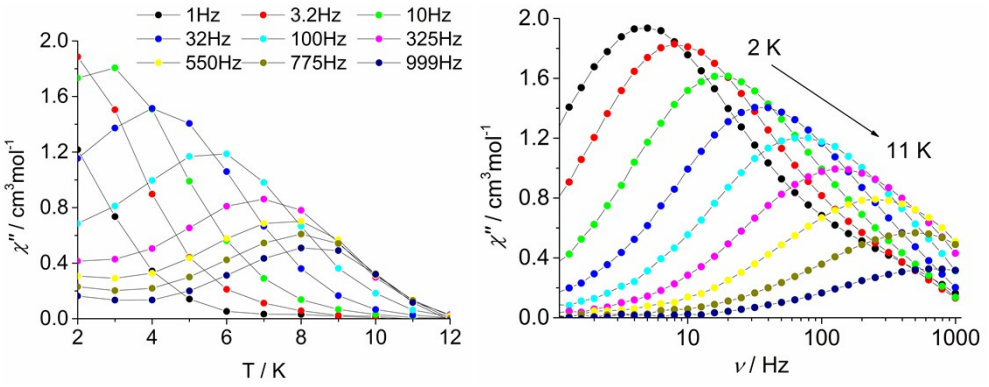

Fig. S32. Temperature dependence of the out-of-phase (χ'') ac susceptibility (left) and frequency dependence of the out-of-phase (χ'') ac susceptibility (right) of complex **1** under 500 Oe.

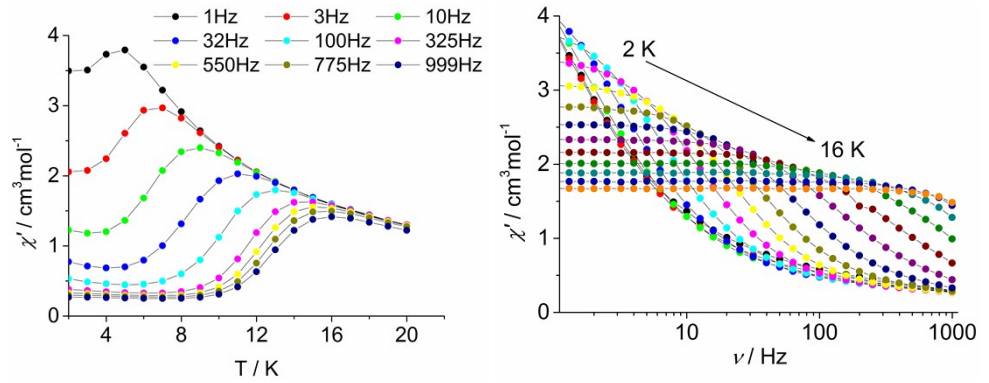

Fig. S33. Temperature dependence of the in-phase (χ') ac susceptibility (left) and frequency dependence of the in-phase (χ') ac susceptibility (right) of complex **2** under 1100 Oe.

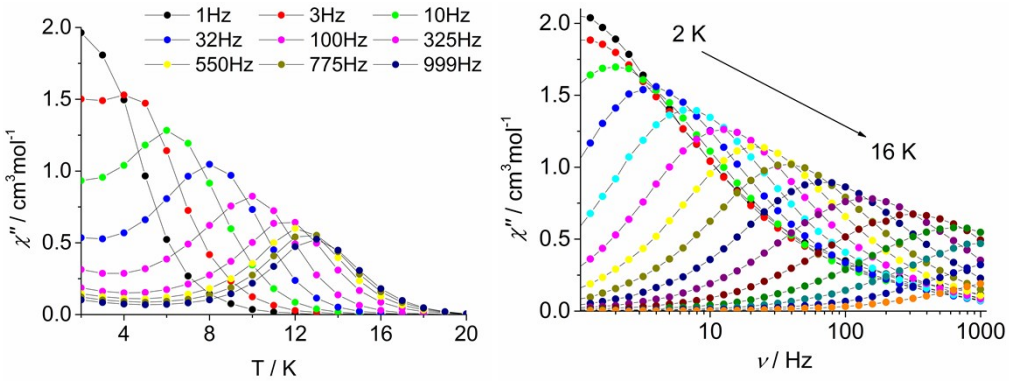

Fig. S34. Temperature dependence of the out-of-phase (χ'') ac susceptibility (left) and frequency dependence of the out-of-phase (χ'') ac susceptibility (right) of complex **2** under 1100 Oe.

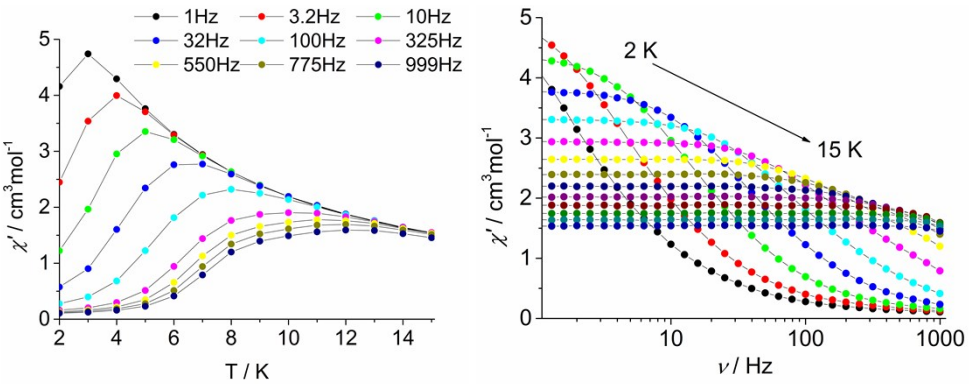

Fig. S35. Temperature dependence of the in-phase (χ') ac susceptibility (left) and frequency dependence of the in-phase (χ') ac susceptibility (right) of complex **3** under 900 Oe.

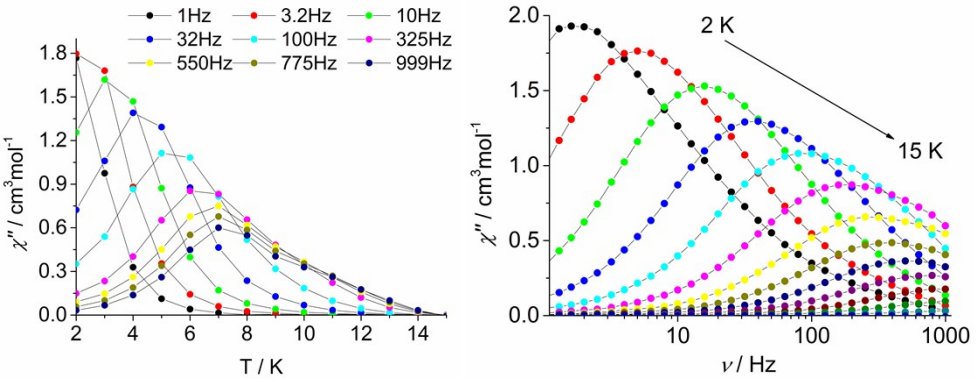

Fig. S36. Temperature dependence of the out-of-phase (χ'') ac susceptibility (left) and frequency dependence of the out-of-phase (χ'') ac susceptibility (right) of complex **3** under 900 Oe.

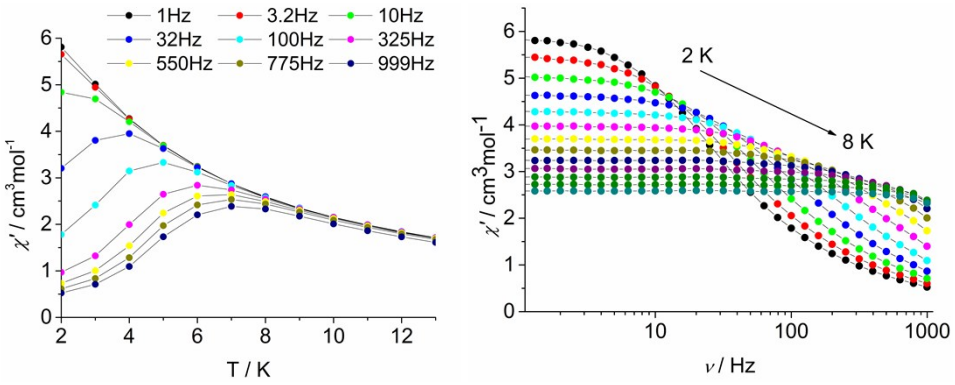

Fig. S37. Temperature dependence of the in-phase (χ') ac susceptibility (left) and frequency dependence of the in-phase (χ') ac susceptibility (right) of complex **4** under 1100 Oe.

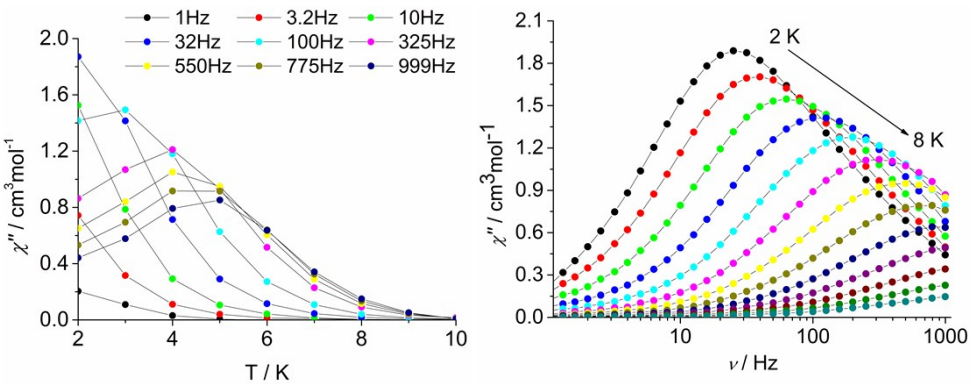

Fig. S38. Temperature dependence of the out-of-phase (χ'') ac susceptibility (left) and frequency dependence of the out-of-phase (χ'') ac susceptibility (right) of complex **4** under 1100 Oe.

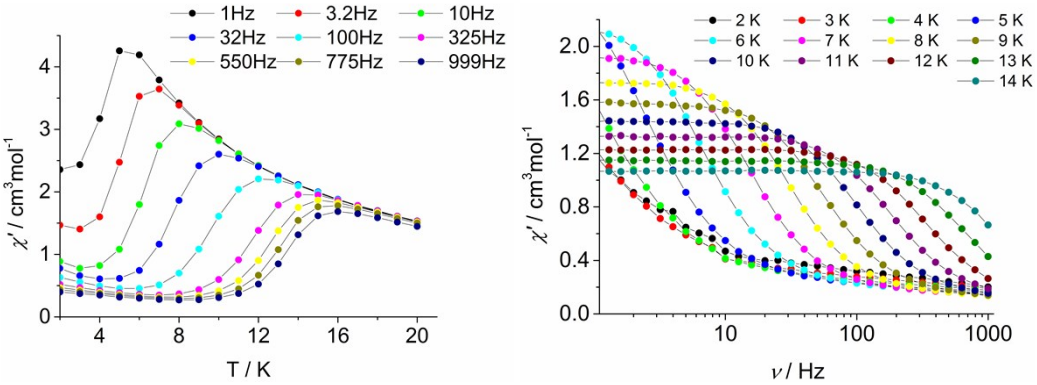

Fig. S39. Temperature dependence of the in-phase (χ') ac susceptibility (left) and frequency dependence of the in-phase (χ') ac susceptibility (right) of complex **5** under 1500 Oe.

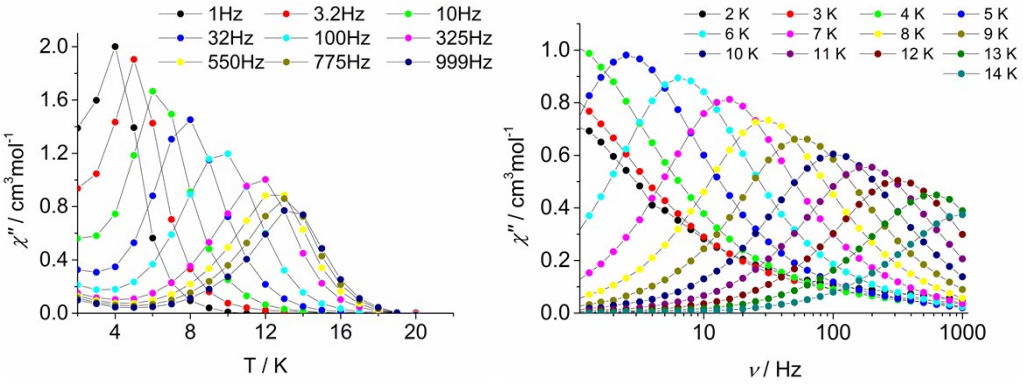

Fig. S40. Temperature dependence of the out-of-phase (χ'') ac susceptibility (left) and frequency dependence of the out-of-phase (χ'') ac susceptibility (right) of complex **5** under 1500 Oe.

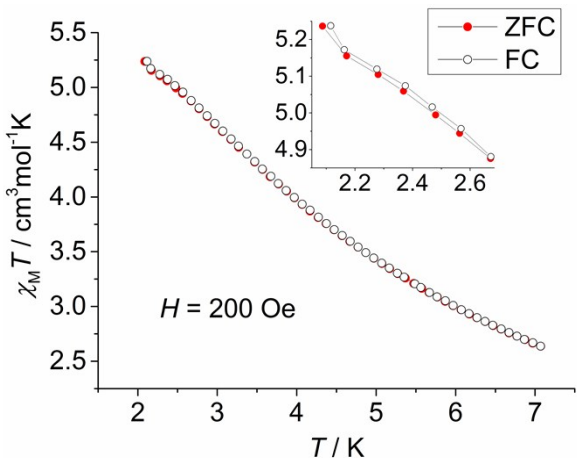

Fig. S41. The zero-field-cooled (ZFC) and field-cooled (FC) susceptibilities at applied dc field for complex **5**.

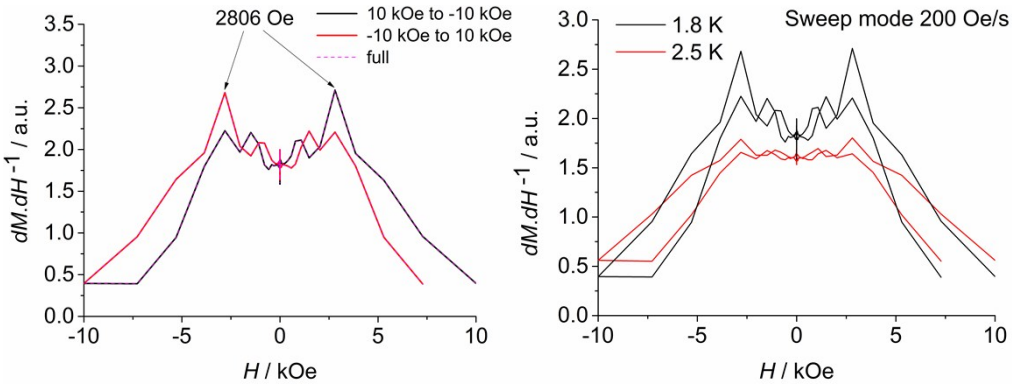

Fig. S42. The first derivative of magnetization (*dM/dH*) of complex **5** versus magnetic field for the curves measured at 1.8 K (left) and different temperature (right) at scan rate of 200 Oe/s, sweep mode.

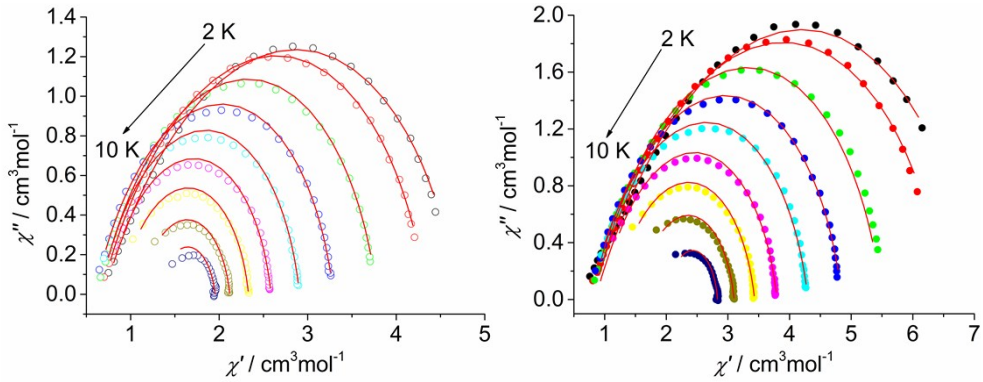

Fig. S43. Cole-Cole (Argand) plot for **1** obtained using the ac susceptibility data. The solid lines correspond to the best fit obtained with a generalized Debye model under zero field (left) and 500 Oe (right).

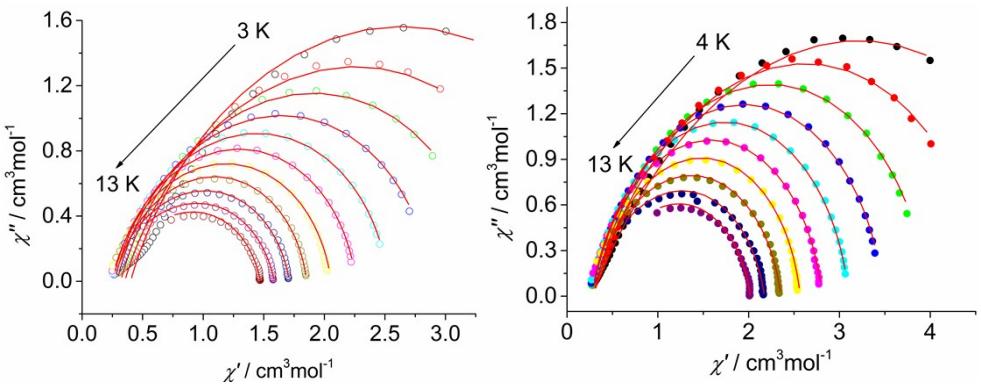

Fig. S44. Cole-Cole (Argand) plot for **2** obtained using the ac susceptibility data. The solid lines correspond to the best fit obtained with a generalized Debye model under zero field (left) and 1100 Oe (right).

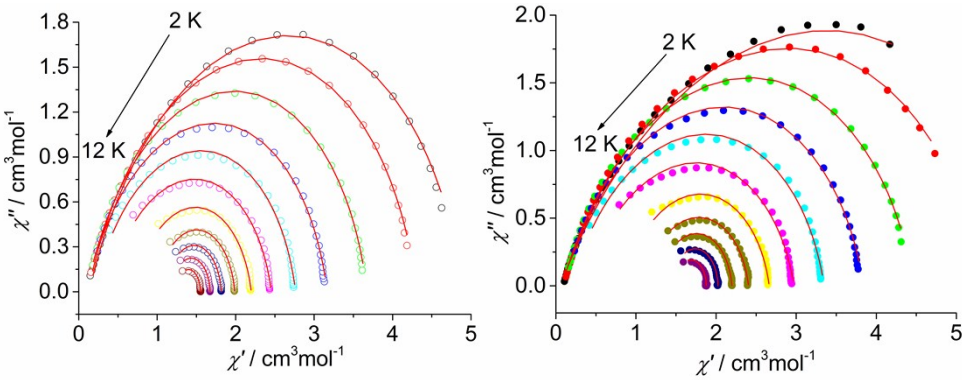

Fig. S45. Cole-Cole (Argand) plot for **3** obtained using the ac susceptibility data. The solid lines correspond to the best fit obtained with a generalized Debye model under zero field (left) and 900 Oe (right).

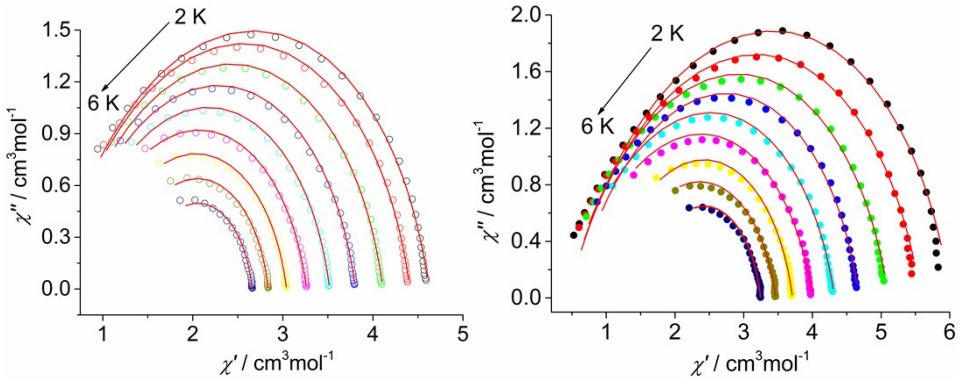

Fig. S46. Cole-Cole (Argand) plot for **4** obtained using the ac susceptibility data. The solid lines correspond to the best fit obtained with a generalized Debye model under zero field (left) and 1100 Oe (right).

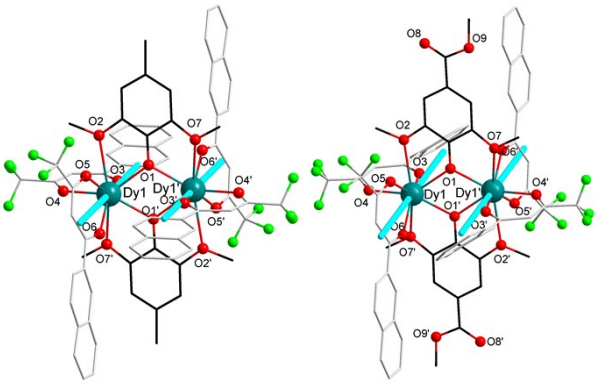

Fig. S47. Orientations of the anisotropy axes for each of the two Dy(III) ions in complexes **1** (left) and **2** (right) as calculated by MAGELLAN.

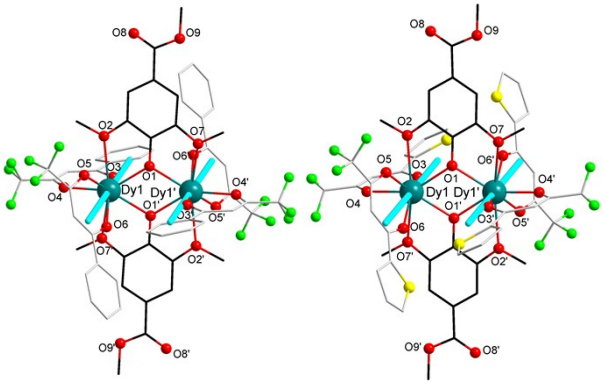

Fig. S48. Orientations of the anisotropy axes for each of the two Dy(III) ions in complexes **3** (left) and **4** (right) as calculated by MAGELLAN.